

RM No. 5E7A08

Authority

*H. L. Dryden* Date *12/29/38*

Dir., Aeronautics  
NACA

**NACA**

By

*PCS*

*see 7118.10-7a*

*CR Rapp*

# RESEARCH MEMORANDUM

for the

Bureau of Aeronautics, Navy Department

ALTITUDE-WIND-TUNNEL INVESTIGATION OF THE  
19B-2, 19B-8, AND 19XB-1 JET-PROPULSION ENGINES

II - ANALYSIS OF TURBINE PERFORMANCE

OF THE 19B-8 ENGINE

By Richard P. Krebs and Frank L. Suozzi

Aircraft Engine Research Laboratory  
Cleveland, Ohio

**CLASSIFICATION CANCELLED**

This document contains classified information affecting the National Defense of the United States within the meaning of the Espionage Laws, Title 18, United States Code, Sections 793 and 794, and the transmission or the revelation of its contents in any manner to an unauthorized person is prohibited by law. Information so classified may be reported only to persons in the military and naval Services of the United States, and to civilian officers and employees of the Federal Government who have a legitimate interest therein, and to persons who have a legitimate interest therein, and to persons who of necessity must be informed thereof.

*H. L. Dryden* 6-5-53

NACA stamp

TECHNICAL EDITING

14/14

Restriction/Classification Cancelled

**NATIONAL ADVISORY COMMITTEE  
FOR AERONAUTICS**

WASHINGTON

JANUARY 20 1947

To be returned to  
the files of the National  
Advisory Committee

for Aeronautics  
Washington, D. C.

**CLASSIFICATION CANCELLED**

13

~~CONFIDENTIAL~~  
~~CLASSIFICATION CANCELLED~~

NATIONAL ADVISORY COMMITTEE FOR AERONAUTICS

RESEARCH MEMORANDUM

for the

Bureau of Aeronautics, Navy Department

ALTITUDE-WIND-TUNNEL INVESTIGATION OF THE

19B-2, 19B-8, AND 19XB-1 JET-PROPULSION ENGINES

II - ANALYSIS OF TURBINE PERFORMANCE

OF THE 19B-8 ENGINE

By Richard P. Krebs and Frank L. Suozzi

SUMMARY

Performance characteristics of the turbine in the 19B-8 jet-propulsion engine were determined from an investigation of the complete engine in the Cleveland altitude wind tunnel. The investigation covered a range of simulated altitudes from 5000 to 30,000 feet and flight Mach numbers from 0.05 to 0.46 for various tail-cone positions over the entire operable range of engine speeds.

The characteristics of the turbine are presented as functions of the total-pressure ratio across the turbine and the turbine speed and the gas flow corrected to NACA standard atmospheric conditions at sea level. The effect of changes in altitude, flight Mach number, and tail-cone position on turbine performance is discussed.

The turbine efficiency with the tail cone in varied from a maximum of 80.5 percent to a minimum of 75 percent over a range of engine speeds from 7500 to 17,500 rpm at a flight Mach number of 0.055. Turbine efficiency was unaffected by changes in altitude up to 15,000 feet but was a function of tail-cone position and flight Mach number. Decreasing the tail-pipe-nozzle outlet area 21 percent reduced the turbine efficiency between 2 and 4.5 percent. The turbine efficiency increased between 1.5 and 3 percent as the flight Mach number changed from 0.055 to 0.297.

~~CONFIDENTIAL~~  
~~CLASSIFICATION CANCELLED~~

## INTRODUCTION

An investigation of the altitude performance and the operational characteristics of the 19B-2, 19B-8, and 19XB-1 jet-propulsion engines has been conducted in the Cleveland altitude wind tunnel at the request of the Bureau of Aeronautics, Navy Department. A summary of the operational characteristics of the three engines is given in reference 1.

The effects of altitude, tail-cone position, and flight Mach number on the performance of the turbine in the 19B-8 engine are given. Data for computing turbine performance were taken from tests on the complete engine. These tests were conducted over a range of simulated altitudes from 5000 to 30,000 feet and flight Mach numbers from 0.05 to 0.46 for various tail-cone positions.

## DESCRIPTION OF TURBINE AND EXHAUST NOZZLE

The 19B-8 engine has a single-stage turbine (fig. 1), which delivers approximately 2000 horsepower at rated engine conditions (17,500 rpm at NACA standard atmospheric conditions at sea level).

The turbine rotor has an outside diameter of  $16\frac{1}{8}$  inches. The rotor is overhung on the shaft, which is supported by two bearings in front of the rotor: a thrust journal bearing located  $22\frac{9}{16}$  inches from the center plane of the rotor, and a plain journal bearing  $5\frac{13}{16}$  inches from the same plane. Both bearings are lubricated by a pressurized oil system. The rotor-hub diameter is 10 inches and the thickness decreases from approximately  $3\frac{1}{2}$  inches at the shaft to  $2\frac{1}{16}$  inches at the periphery.

The ends of the bulb-type roots of the 32 solid blades are peened over to lock them into the hub. The blade length is  $3\frac{1}{16}$  inches; the chord decreases from  $2\frac{1}{16}$  inches at the root to  $1\frac{13}{32}$  inches at the tip. The radial tip clearance for the wheel is 0.078 inch.

The turbine nozzle (fig. 2) consists of 44 solid, equally spaced blades that fit into slots in two shroud rings. The outer shroud ring is  $16\frac{9}{16}$  inches in diameter and the inner shroud ring,  $9\frac{13}{16}$  inches. The blades are of constant width and thickness and are so set that the chord line makes an angle of approximately  $41^\circ$  with the plane of rotation of the turbine.

The exhaust nozzle has a movable inner cone actuated by a hydraulic cylinder mounted on the outside of the combustion chamber. Moving the inner cone from the "in" position to the "4-inches-out" position decreases the tail-pipe-nozzle outlet area, measured in a plane perpendicular to the center line of the engine, from approximately 135 to 106 square inches.

#### INSTRUMENTATION

The 19B-8 jet-propulsion engine was instrumented at the stations shown in figure 3. Details of the instrumentation at those stations from which data for this report were taken were as follows (all instrumentation was unshielded unless otherwise noted):

The cowl inlet, station 1, was instrumented with sixteen total-pressure tubes, nine static-pressure tubes, and four iron-constantan thermocouples. The arrangement of the pressure tubes and thermocouples is shown in figure 4.

The instrumentation at station 2, the compressor inlet, was carried by four rakes set at  $45^\circ$  to the center line of the engine. These rakes contained twelve total-pressure tubes and eight iron-constantan thermocouples. Four wall static-pressure orifices were also provided at this station.

At station 3, the compressor outlet, the instrumentation was mounted on four rakes set at right angles to one another. The rakes contained six total-pressure tubes, two static-pressure tubes, and four iron-constantan thermocouples. Four wall static-pressure orifices were also provided.

At station 4, the turbine inlet, total pressure was measured by a Westinghouse integrating rake. Viewed from the front of the engine, the location of the rake was in the lower right quadrant  $17.5^\circ$  from the horizontal diameter and  $3\frac{5}{16}$  inches ahead of the turbine. The rake is shown and its position indicated in figure 5.

The instrumentation at the turbine outlet, station 5, consisted of twelve shielded total-pressure tubes and eight chromel-alumel thermocouples mounted as shown in figure 6. Four wall static-pressure orifices were also installed at this station.

## RANGE OF INVESTIGATION

The engine performance was investigated over a range of simulated altitudes from 5000 to 30,000 feet and flight Mach numbers from 0.05 to 0.46 with the engine tail cone in over the entire operable range of engine speeds. The range with the tail cone 4 inches out was restricted by the necessity of keeping the turbine-inlet temperature below 1960° R. The tunnel temperatures were maintained at approximately NACA standard atmospheric conditions for each altitude.

## SYMBOLS

The following symbols and necessary values are used in the computations:

- A cross-sectional area, square feet
- $c_p$  specific heat at constant pressure, Btu per pound °R
- g ratio of absolute to gravitational units of mass, 32.17
- J mechanical equivalent of heat, 778 foot-pounds per Btu
- N engine speed, rpm
- P total pressure, pounds per square foot
- p static pressure, pounds per square foot
- T total temperature, °R
- $T_i$  indicated temperature, °R
- t static temperature, °R
- V velocity, feet per second
- $W_a$  air flow, pounds per second
- $W_f$  fuel flow, pounds per second
- $W_g$  gas flow, pounds per second
- $\alpha$  thermocouple impact-recovery factor, 0.85
- $\gamma$  ratio of specific heats

- $\delta_4$  pressure-correction factor,  $P_4/2116$ ; turbine-inlet total pressure divided by NACA standard atmospheric pressure at sea level
- $\eta_t$  turbine efficiency
- $\theta_4$  temperature-correction factor,  $\gamma_4 T_4 / (1.4 \times 519)$ ; product of  $\gamma$  and turbine-inlet total temperature divided by product of  $\gamma$  and total temperature at NACA standard atmospheric conditions at sea level
- $\rho$  density, slugs per cubic foot

## Subscripts:

- c compressor
- t turbine
- 0 free-stream or ambient
- 1 cowl inlet
- 4 turbine inlet
- 5 turbine outlet

## METHODS OF COMPUTATION

## Gas Flow

The gas flow was found by adding the fuel flow to the air flow:

$$W_g = W_f + W_a$$

Air flow was determined from pressure and temperature measurements at the cowl inlet, station 1, by

$$W_a = \rho_1 A_1 V_1 = \rho_1 A_1 \sqrt{2Jg c_{p,1} t_1 \left[ \left( \frac{P_1}{P_1} \right)^{\frac{\gamma_1 - 1}{\gamma_1}} - 1 \right]}$$

## Temperatures

Static temperature was calculated from the indicated temperature by

$$t = \frac{T_i}{1 + \alpha \left[ \left( \frac{P}{p} \right)^\gamma - 1 \right]}$$

The thermocouple impact-recovery factor  $\alpha$  was determined from calibration tests and was found to be 0.85.

Total temperature was determined by the adiabatic relation

$$\frac{T}{t} = \left( \frac{P}{p} \right)^\gamma$$

## Efficiency

Turbine efficiency, based on the total-pressure ratio across the turbine with bearing friction losses, power required to drive the accessories, and compressor and turbine thermal losses neglected, was defined by

$$\eta_t = \frac{\Delta T_t}{T_4 \left[ 1 - \left( \frac{P_5}{P_4} \right)^\gamma \right]}$$

The enthalpy rise across the compressor was assumed equal to the enthalpy drop across the turbine and the total-temperature drop across the turbine was obtained from

$$\Delta T_t = \frac{\Delta T_c c_{p,c}}{\left( 1 + \frac{W_f}{W_a} \right) c_{p,t}}$$

The total temperature at the turbine inlet was computed from

$$T_4 = \Delta T_t + T_5$$

The value of  $\gamma_t$  was determined from a curve using values of fuel-air ratio and an average of the turbine-inlet and turbine-outlet temperatures. The curve was based on a hydrogen-carbon ratio of 0.170 and a combustion efficiency of 98 percent.

Turbine efficiency was determined from a plot of  $1 - \left(\frac{P_5}{P_4}\right)^{\frac{\gamma-1}{\gamma}}$  against  $\Delta T_t/T_4$ . The values of efficiency presented were obtained from a curve faired through the data points of this plot.

### RESULTS AND DISCUSSION

The method of presentation of the turbine data used in this report follows the same pattern as that used in referencé 2. Turbine performance is shown by plots of turbine pressure ratio  $P_4/P_5$  against corrected engine speed  $N/\sqrt{\theta_4}$  and corrected gas flow  $\frac{W_g \sqrt{\theta_4}}{\delta_4 \gamma_4 / 1.4}$ , and turbine efficiency  $\eta_t$  plotted against turbine pressure ratio. The plot of turbine pressure ratio against corrected gas flow is designated the turbine operating line.

Each run was made at constant flight Mach number. Because a screen had been inserted at the cowl inlet to protect the engine, the ram-pressure ratio  $P_2/p_0$  decreased as the air flow and the engine speed increased. Curves of the compressor-inlet ram-pressure ratio are given on most of the performance curves.

#### Effect of Altitude

Two plots relating turbine pressure ratio with corrected turbine speed and corrected gas flow for three different simulated altitudes are shown in figure 7. These data were taken with the engine tail cone in at flight Mach numbers between 0.142 and 0.153. The small changes in flight Mach number and ram-pressure ratio were considered insufficient to impair the conclusions drawn on the effect of altitude on turbine performance. Figure 7 shows that a change in simulated altitude from 5000 to 15,000 feet had little effect on the two relations. At a simulated altitude of 25,000 feet, the corrected turbine speed decreases and the corrected gas flow increases from those values obtained at 5000 or 15,000 feet. These differences are probably caused by erratic combustion rather than by any changes in the turbine performance at the high altitude.



The quantity  $1 - \left(\frac{P_5}{P_4}\right)^{\frac{\gamma_t-1}{\gamma_t}}$  is plotted against  $\Delta T_t/T_4$  for three simulated altitudes in figure 8. The turbine efficiency is calculated by dividing  $\Delta T_t/T_4$  by the adiabatic temperature-drop factor. The data points for simulated altitudes of 5000 and 15,000 feet show no change in turbine efficiency with change in altitude.

#### Effect of Tail-Cone Position

The effect of changes in the tail-cone position on turbine performance is shown in figures 9 and 10. The data presented were taken at a simulated altitude of 15,000 feet and a flight Mach number of 0.147. A decrease in tail-pipe-nozzle outlet area decreases the air flow, raises the compressor pressure ratio, increases the temperature differences across both the compressor and turbine, and raises the turbine-inlet temperature. Although the turbine work per pound of gas increases, the turbine-inlet temperature increases sufficiently to cause a drop in the turbine pressure ratio. Typical values of turbine-inlet temperature, turbine pressure ratio, and temperature drop across the turbine for several engine speeds are shown in the following table:

Tail-cone position	Engine speed (rpm)	Turbine-inlet temperature ( $^{\circ}$ R)	Turbine pressure ratio	Turbine temperature drop ( $^{\circ}$ R)
In 4 in. out	14,400	1427	1.890	165
		1642	1.832	168
In 4 in. out	15,517	1478	1.965	188
		1816	1.890	198
In 4 in. out	16,514	1578	2.066	210
		2025	1.945	221

When the tail cone is moved out, the change in the corrected turbine speed is greater than the change in the pressure ratio; thus the curve of the pressure ratio plotted against the corrected turbine speed shifts to the left (fig. 9(a)).

Reference 2 established that, when the velocity in the turbine nozzle was sonic (that is, the pressure ratio across the nozzle was greater than critical, 1.84 to 1.89, depending on the value of  $\gamma_4$ ), the turbine operating line was affected only by changes in  $\gamma_4$ . Because the turbine in the 19B-8 engine is a reaction design, the static-pressure drops through the rotor and the turbine pressure ratio may be considerably higher than the critical value before sonic flow is established in the turbine nozzle. When the tail cone is moved out, the turbine-inlet temperature is increased by the addition of more fuel and  $\gamma_4$  is reduced by both the increase in temperature and fuel-air ratio. The amount of increase in the corrected gas flow caused by this reduction in  $\gamma_4$  was computed to be 0.3 percent. The turbine operating line shifts toward the higher corrected gas flows by about 0.8 percent (fig. 9(b)).

Turbine efficiency is plotted against turbine pressure ratio for two different tail-cone positions and a flight Mach number of 0.147 in figure 10. The turbine efficiency varies from a maximum of 80.5 percent to a minimum of 76.5 percent over a range of turbine pressure ratios from 1.2 to 2.1 corresponding to engine speeds from 7500 to 17,500 rpm with the tail cone in. The efficiencies are from 2 to 4.5 percent lower when the tail cone is moved out and the tail-pipe-nozzle outlet area is thus decreased 21 percent.

The curves in figure 10 have shapes different from efficiency curves for the turbines of other jet-propulsion engines investigated in the altitude wind tunnel. For the other turbines, the efficiencies are low at low turbine pressure ratios, rise to a maximum near the critical turbine pressure ratio, and then decrease as the pressure ratio is further increased. For such a turbine, the operating lines lie to the left of the region of maximum turbine efficiency. (See fig. 8, reference 2.) For the turbine in the 19B-8 engine, however, the operating lines are to the right of the region of maximum turbine efficiency (fig. 11). If the range of tests were extended to higher or lower turbine pressure ratios, the efficiencies would begin to decrease. The efficiency curve for the tail cone 4 inches out exhibits this tendency at the low turbine pressure ratios (fig. 10)).

#### Effect of Flight Mach Number

The effect of changes in flight Mach number on turbine-inlet temperature, turbine pressure ratio, and the temperature drop across the turbine for several engine speeds is shown in the following table:

Flight Mach number	Engine speed (rpm)	Turbine-inlet temperature ( $^{\circ}$ R)	Turbine pressure ratio	Turbine temperature drop ( $^{\circ}$ R)
0.055	14,400	1510	1.860	161
.142		1472	1.838	164
.297		1420	1.800	160
0.055	15,517	1567	1.955	187
.142		1510	1.976	187
.297		1509	1.930	182
0.055	17,000	1619	2.108	222
.142		1635	2.082	220
.297		1616	2.070	217

Although the table contains small inconsistencies, the data indicate that probably an increase in flight Mach number decreases the turbine-inlet temperature, the turbine pressure ratio, and the temperature drop across the turbine. Because the temperature drop across the turbine decreases, the work done by the turbine per pound of gas also decreases as the flight Mach number increases. Low turbine-inlet temperature increases the corrected turbine speed and the curves in figure 12(a) are shifted to the right as the flight Mach number is increased.

The shift in the three operating lines, shown in figure 12(b), is attributable to faulty measurements, probably of the air flow. Air flow was measured at the cowl inlet by the rakes shown in figure 4. No total-pressure tubes were situated near enough the outside of the inlet to detect a boundary layer. A change in boundary-layer thickness of about 0.2 inch would account for the shift in the operating lines shown in figure 12(b).

With the tail cone in, the turbine efficiency varies from a maximum of 80.5 percent to a minimum of 75 percent over a range of turbine pressure ratios from 1.2 to 2.1 corresponding to engine speeds from 7500 to 17,500 rpm at a flight Mach number of 0.055 and is increased by an increase in flight Mach number. This effect is illustrated in figure 13 where turbine efficiency is plotted against turbine pressure ratio for several flight Mach numbers. The data were taken at a simulated altitude of 5000 feet with the tail cone in. Efficiencies are increased between 1.5 and 3 percent when the flight Mach number is increased from 0.055 to 0.297.

## SUMMARY OF RESULTS

An investigation of the turbine performance of the 19B-8 jet-propulsion engine over a range of simulated altitudes from 5000 to 30,000 feet and flight Mach numbers from 0.05 to 0.46 gave the following results:

1. The turbine efficiency (uncorrected for bearing-friction losses, compressor and turbine thermal losses, and the power required to drive the accessories) varied from a maximum of 80.5 percent to a minimum of 75 percent as the turbine pressure ratio changed from 1.2 to 2.1 corresponding to a change of engine speed from 7500 to 17,500 rpm at a flight Mach number of 0.055 with the tail cone in.
2. Turbine efficiency was unaffected by changes in altitude up to 15,000 feet.
3. Turbine efficiency decreased from 2 to 4.5 percent when the tail-pipe-nozzle outlet area was decreased 21 percent.
4. Turbine efficiency increased from 1.5 to 3 percent when the flight Mach number was increased from 0.055 to 0.297.

Aircraft Engine Research Laboratory,  
National Advisory Committee for Aeronautics,  
Cleveland, Ohio.

*Richard P. Krebs*  
Richard P. Krebs,  
Physicist.

Frank L. Suozzi,  
Aeronautical Engineer.

Approved:

*Newell D. Sanders*

Newell D. Sanders,  
Mechanical Engineer.

*Abe Silverstein*  
Abe Silverstein,  
Aeronautical Engineer.

lrp

## REFERENCES

1. Fleming, William A.: Altitude-Wind-Tunnel Investigation of the Westinghouse 19B-2, 19B-8, and 19XB-1 Jet-Propulsion Engines. I - Operational Characteristics. NACA MR No. E6E06, Bur. Aero., 1946.
2. Krebs, Richard P., and Hensley, Reece V.: Altitude-Wind-Tunnel Tests of the General Electric TG-180 Jet-Propulsion Engine. V - Analysis of Turbine Performance. NACA MR No. E6F11, Army Air Forces, 1946.

NACA  
C-14565  
3-26-46

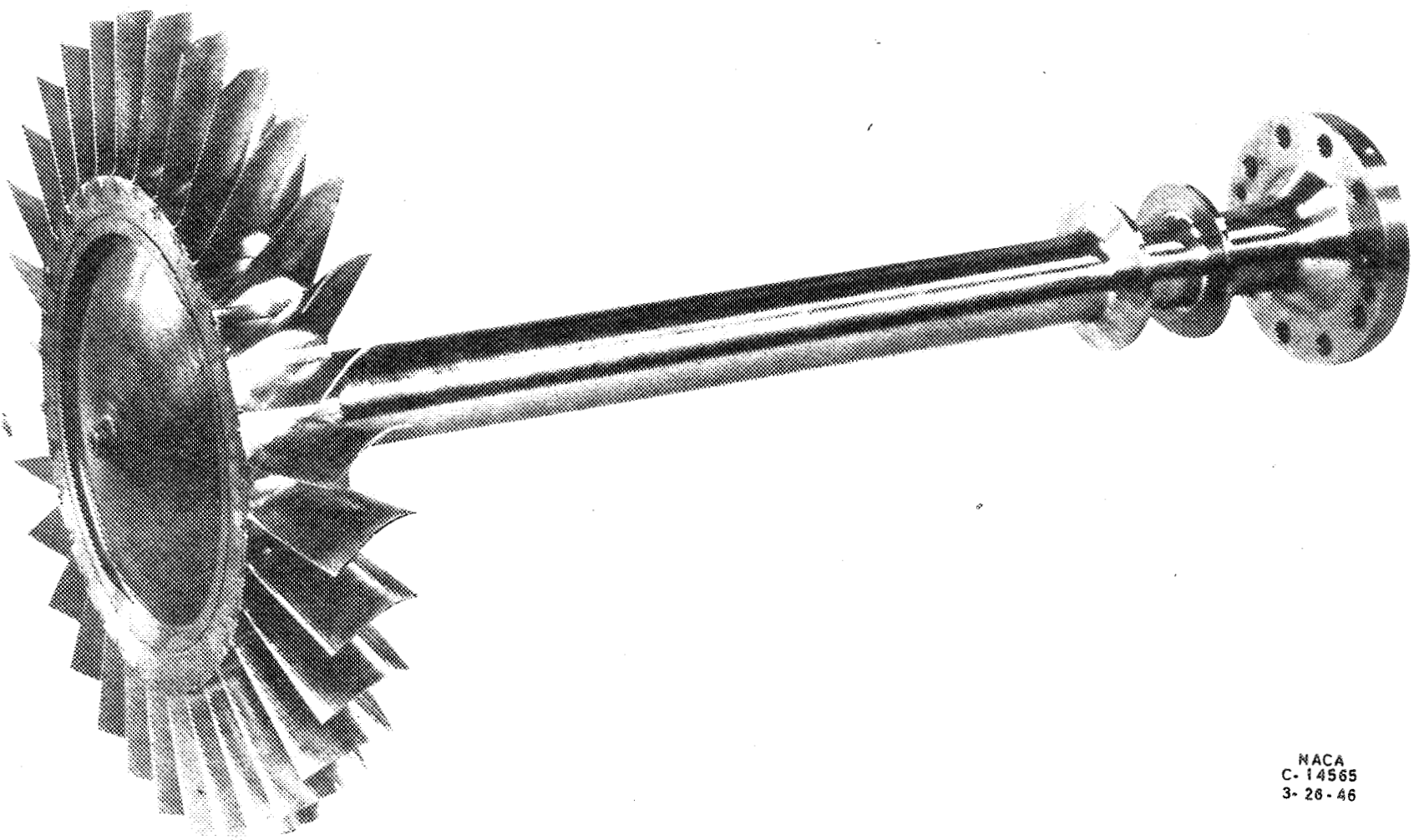
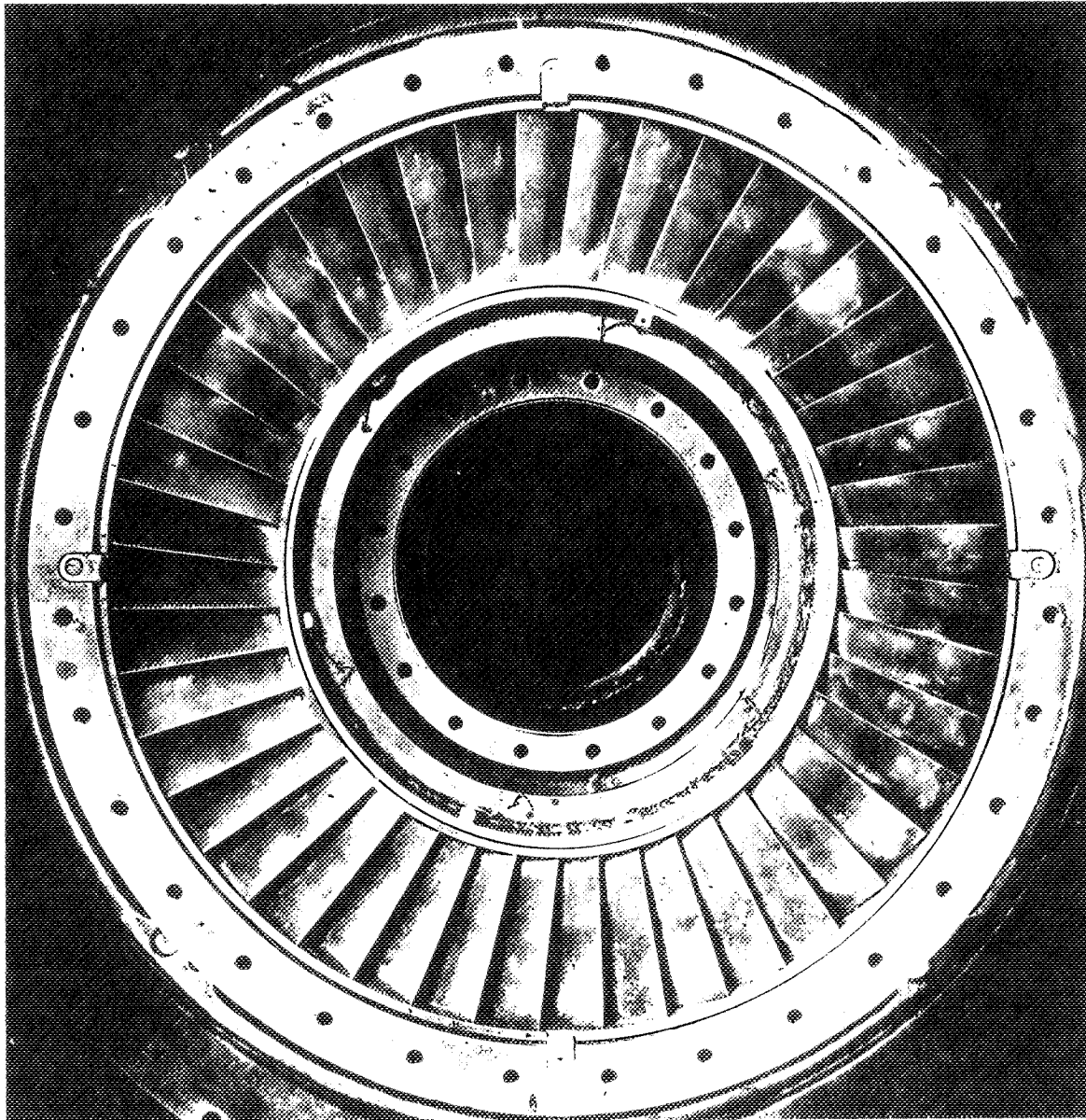
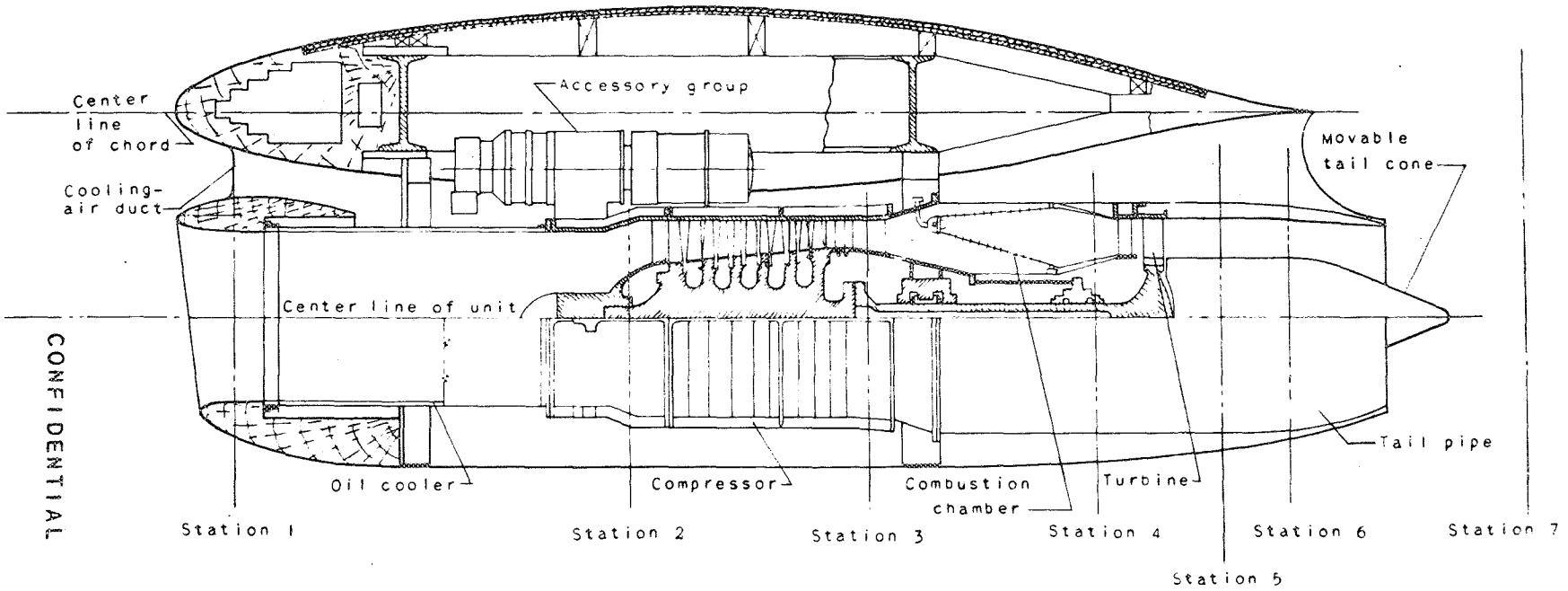


Figure 1. - Single-stage turbine rotor and shaft of 19B-8 jet-propulsion engine.



NACA  
C-14566  
3-26-46

Figure 2. - Turbine nozzle of 19B-8 jet-propulsion engine.



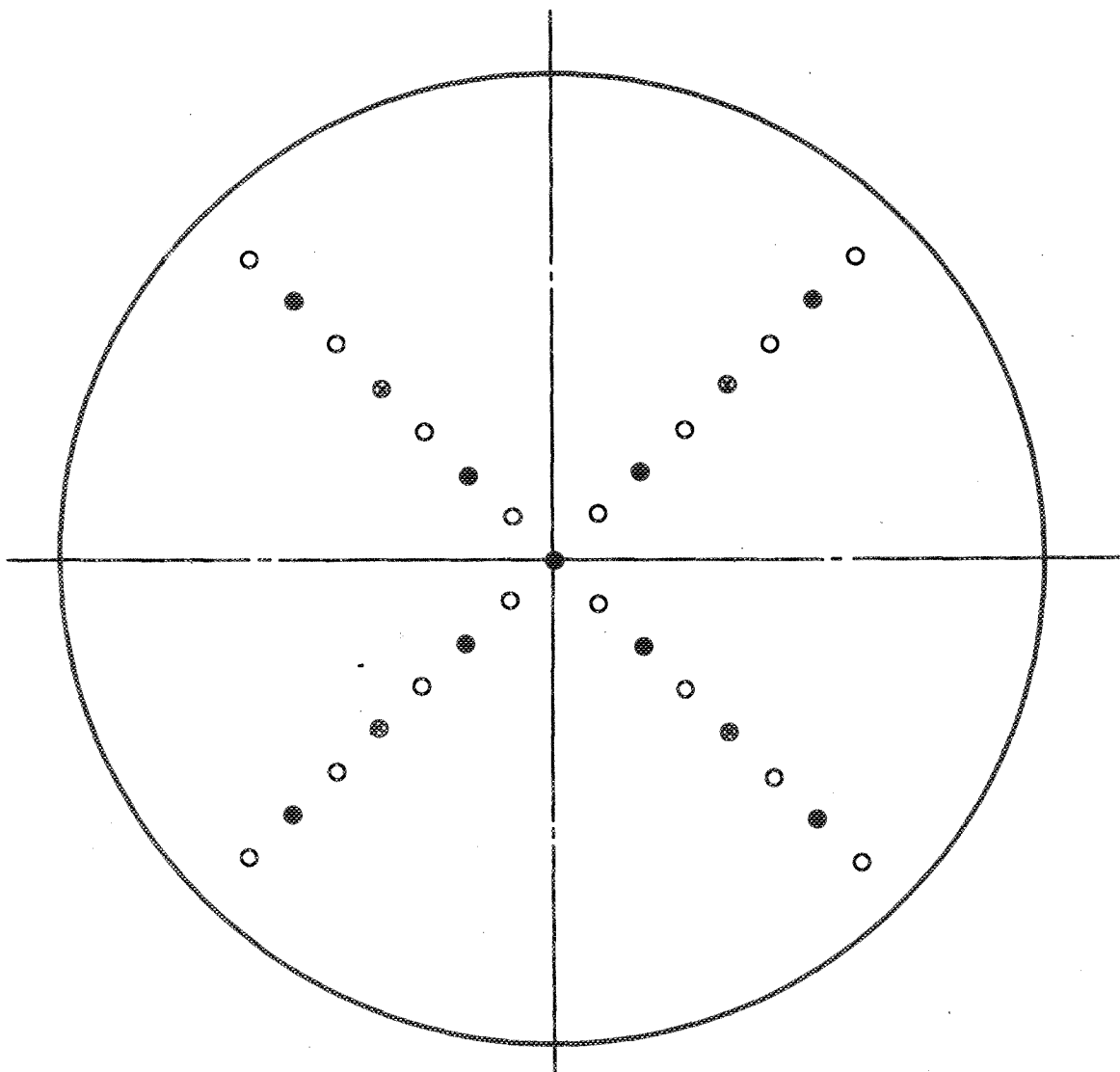
CONFIDENTIAL

NATIONAL ADVISORY  
COMMITTEE FOR AERONAUTICS

Figure 3. - Side view of 19B-8 jet-propulsion-engine installation showing measuring stations.



NATIONAL ADVISORY  
COMMITTEE FOR AERONAUTICS



- Total-pressure tube
- Static-pressure tube
- ⊗ Thermocouple

Figure 4.-- Location of instrumentation at cowl inlet, station 1. Plane of survey,  $2\frac{7}{8}$  inches ahead of front flange of oil cooler.

NATIONAL ADVISORY  
COMMITTEE FOR AERONAUTICS

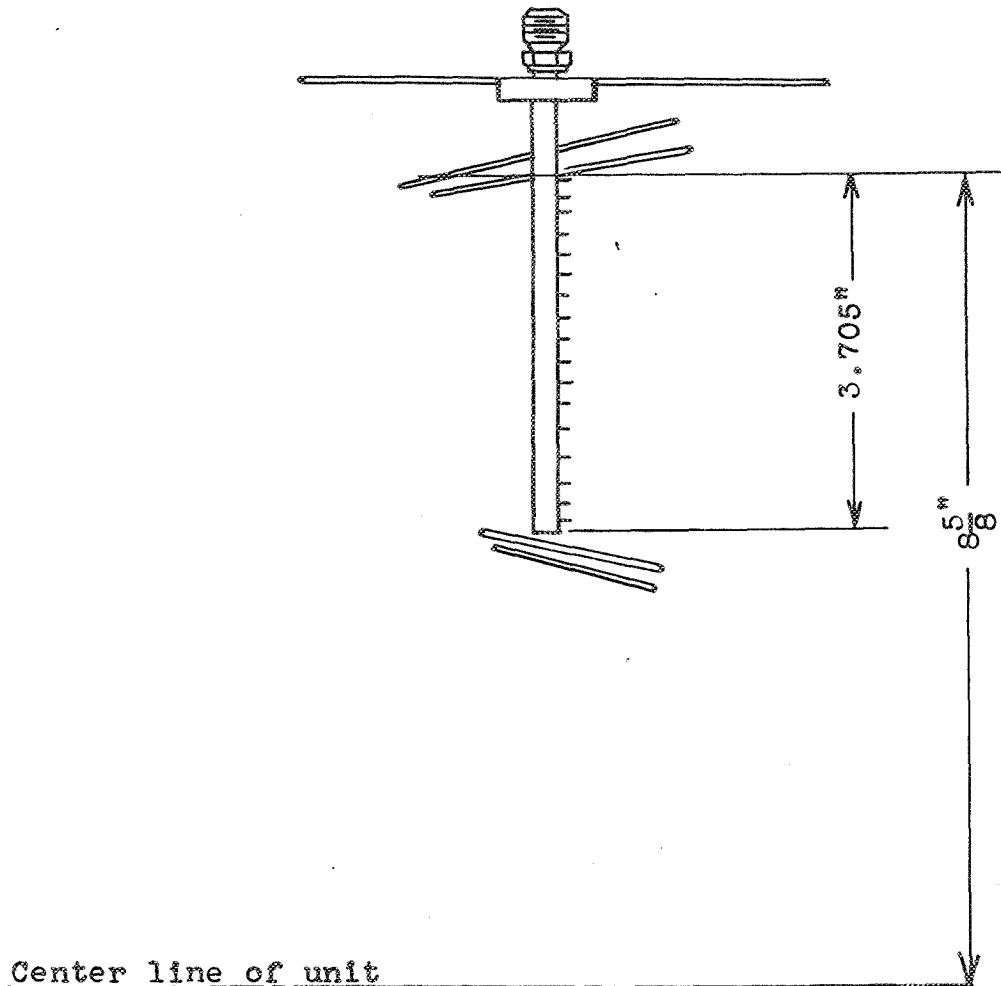
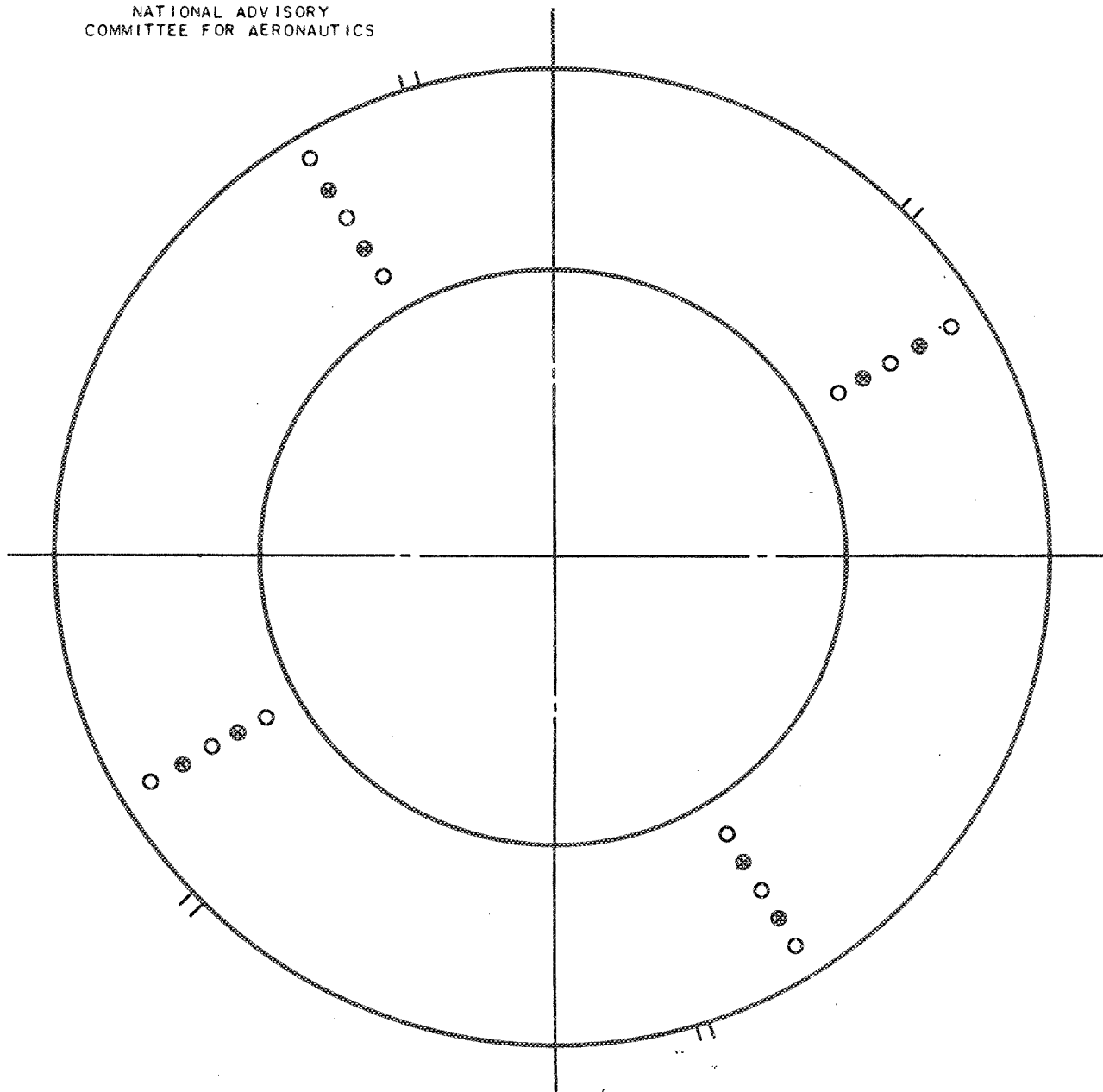


Figure 5.- Westinghouse integrating rake for measuring turbine-inlet total pressure at station 4. Location of rake (viewed in direction of gas flow): lower right quadrant,  $17.5^\circ$  from horizontal diameter,  $\frac{5}{16}$  inches upstream of turbine.

NATIONAL ADVISORY  
COMMITTEE FOR AERONAUTICS

- Total-pressure tube (shielded)
- || Wall static-pressure orifice
- ⊗ Thermocouple

Figure 6.- Location of instrumentation at turbine outlet, station 5. Location of rakes,  $5\frac{5}{8}$  inches behind rear flange of combustion chamber.

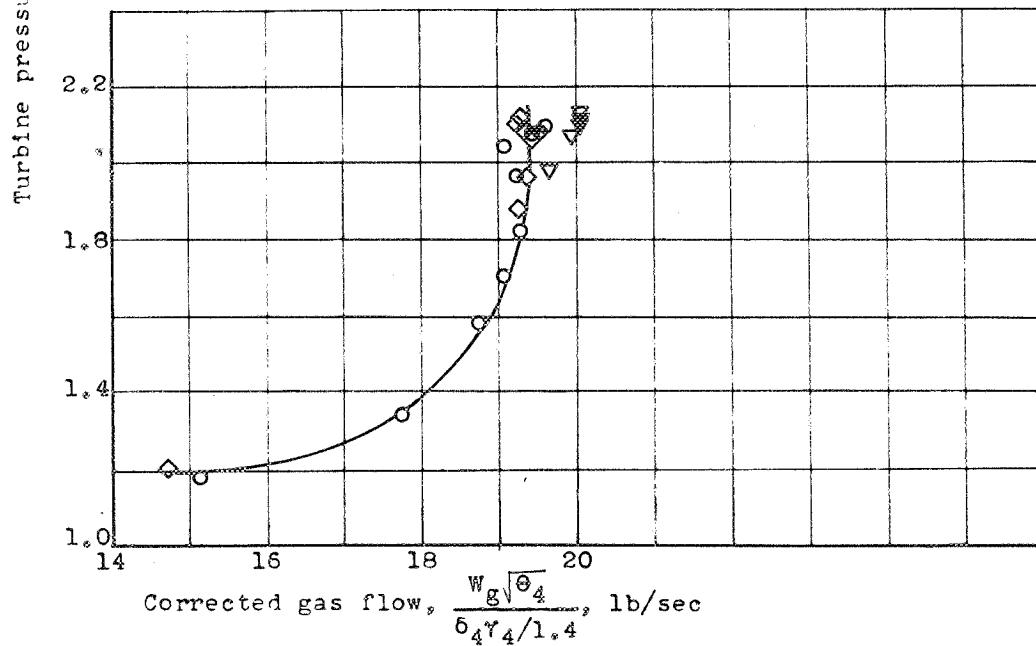
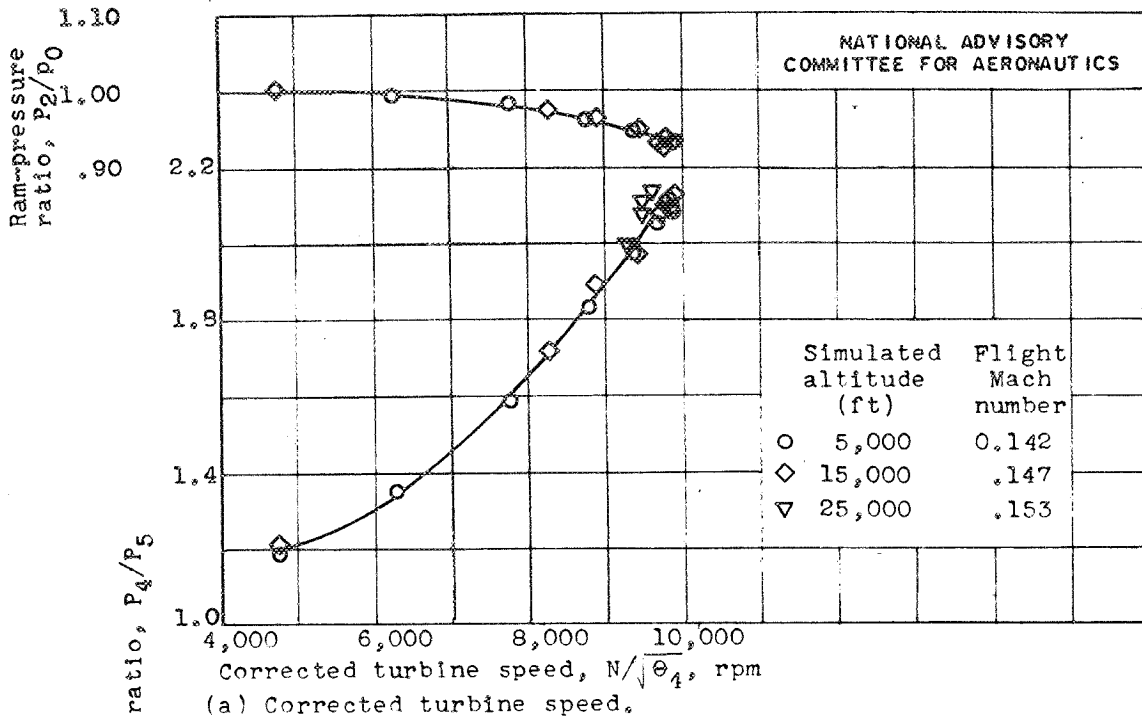


Figure 7.- Effect of altitude on turbine pressure ratio as function of two corrected parameters. Tail cone in. Turbine speed and gas flow corrected to NACA standard atmospheric conditions at sea level.

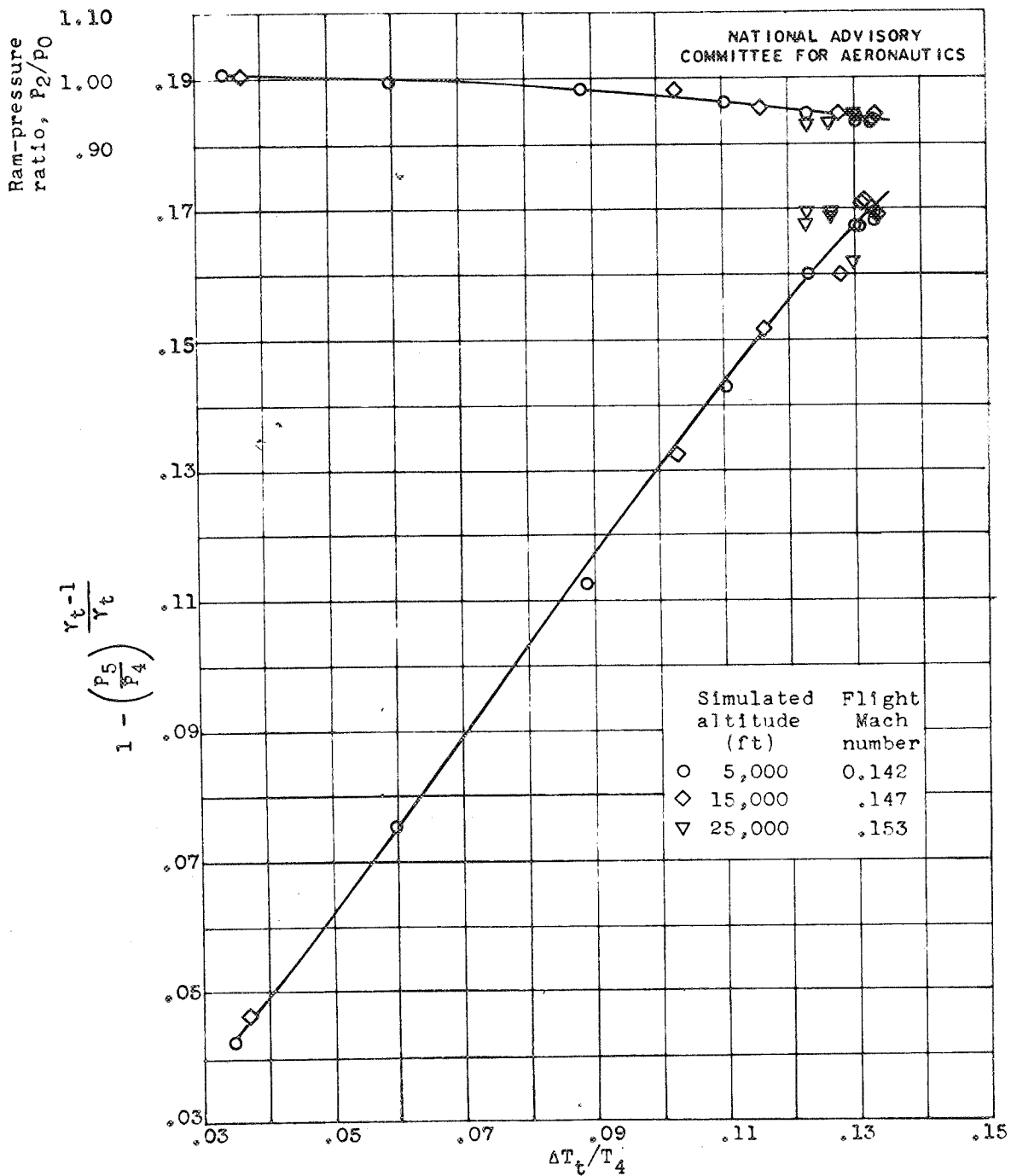


Figure 8.- Plot used in computing turbine efficiency. Tail cone in.

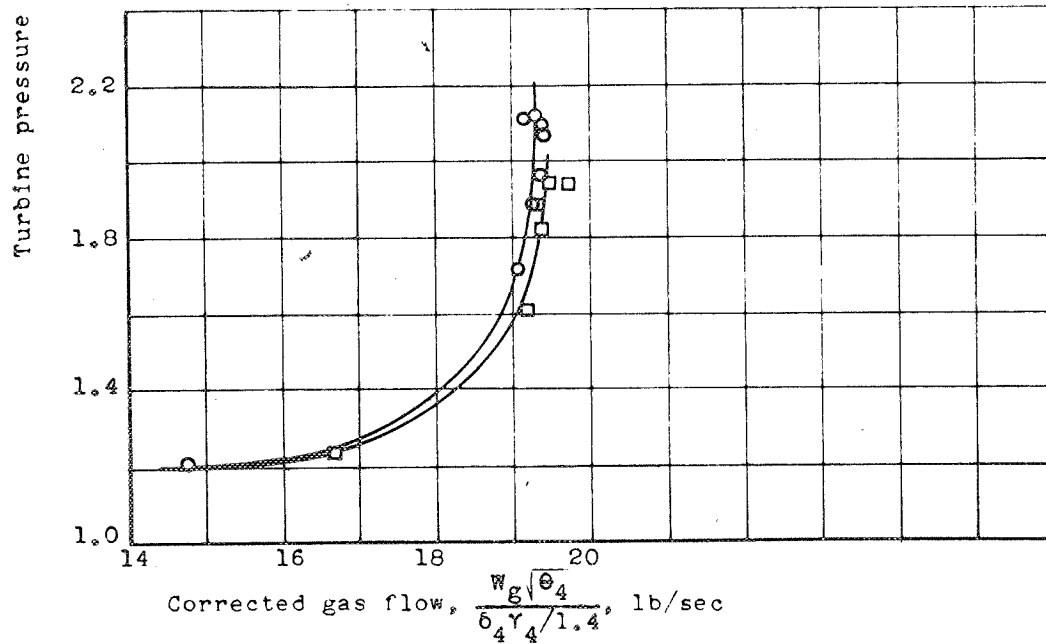
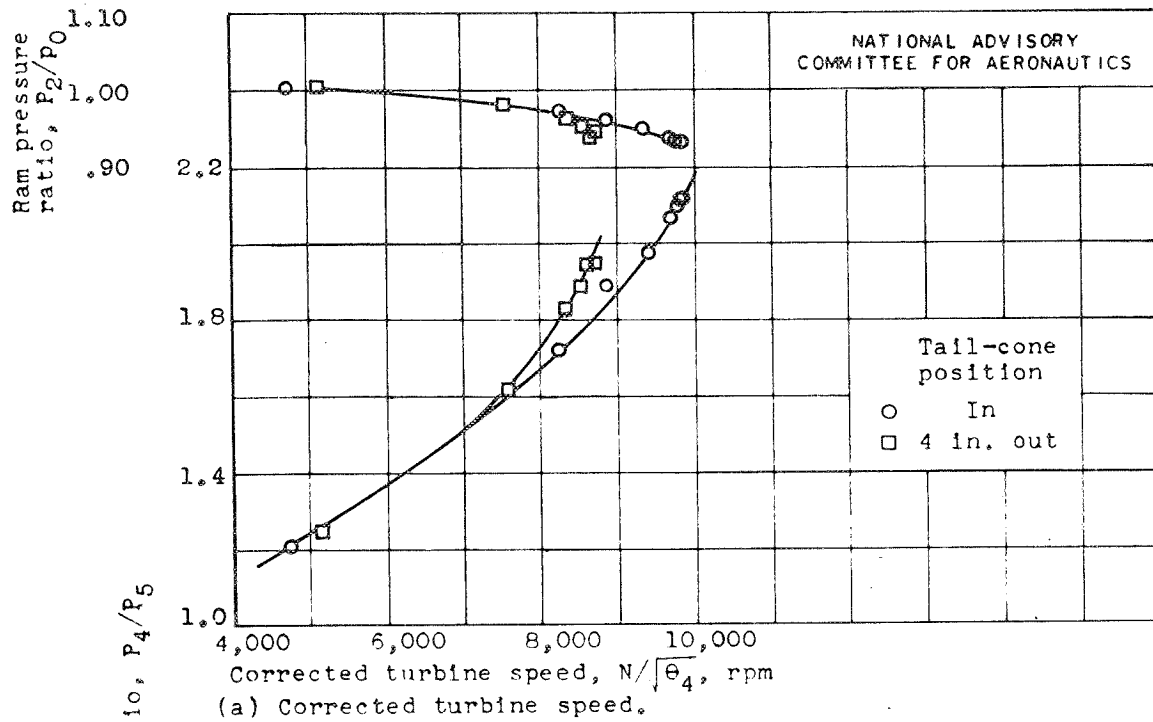


Figure 9.- Effect of tail-cone position on turbine pressure ratio as function of two corrected parameters. Simulated altitude, 15,000 feet; flight Mach number, 0.147. Turbine speed and gas flow corrected to NACA standard atmospheric conditions at sea level.

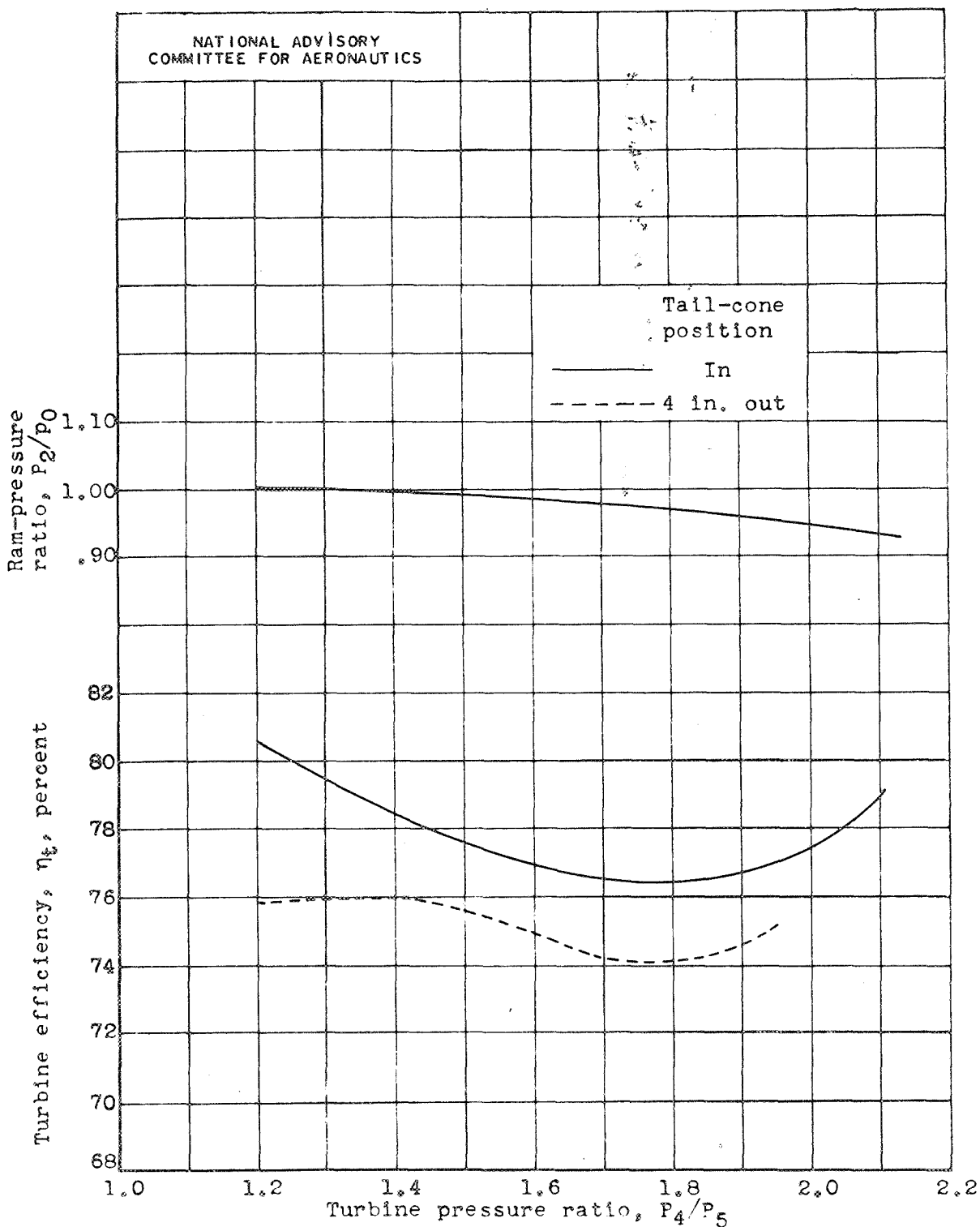


Figure 10.- Effect of tail-cone position on turbine efficiency. Simulated altitude, 15,000 feet; flight Mach number, 0.147.

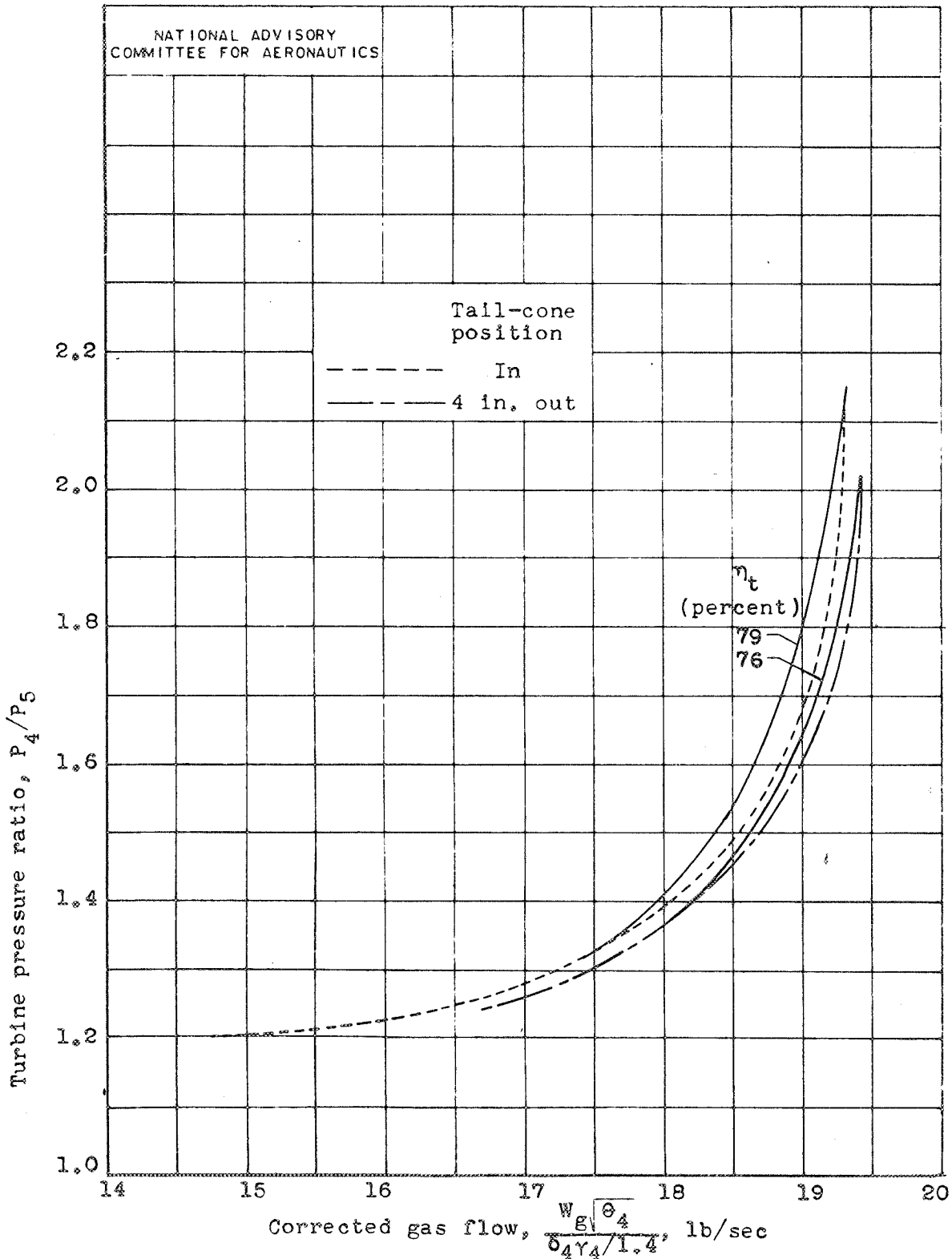


Figure 11.- Efficiency contours plotted on two turbine operating lines. Simulated altitude, 15,000 feet; flight Mach number, 0.147. Gas flow corrected to NACA standard atmospheric conditions at sea level.



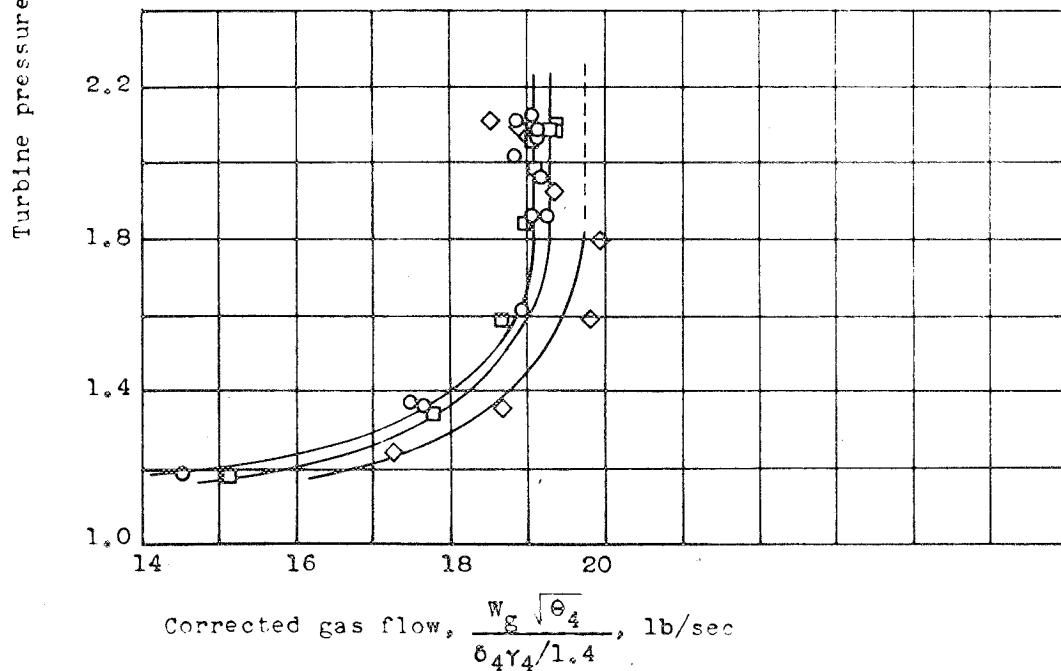
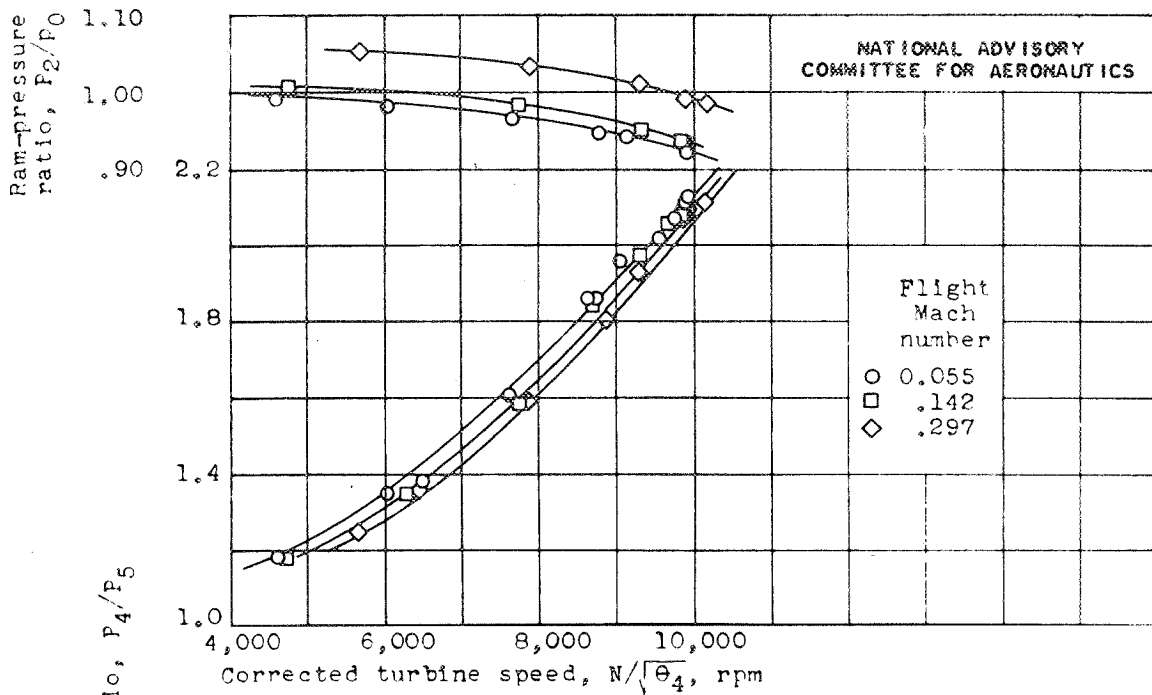


Figure 12.- Effect of flight Mach number on turbine pressure ratio as function of two corrected parameters. Simulated altitude, 5000 feet; tail cone in. Turbine speed and gas flow corrected to NACA standard atmospheric conditions at sea level.

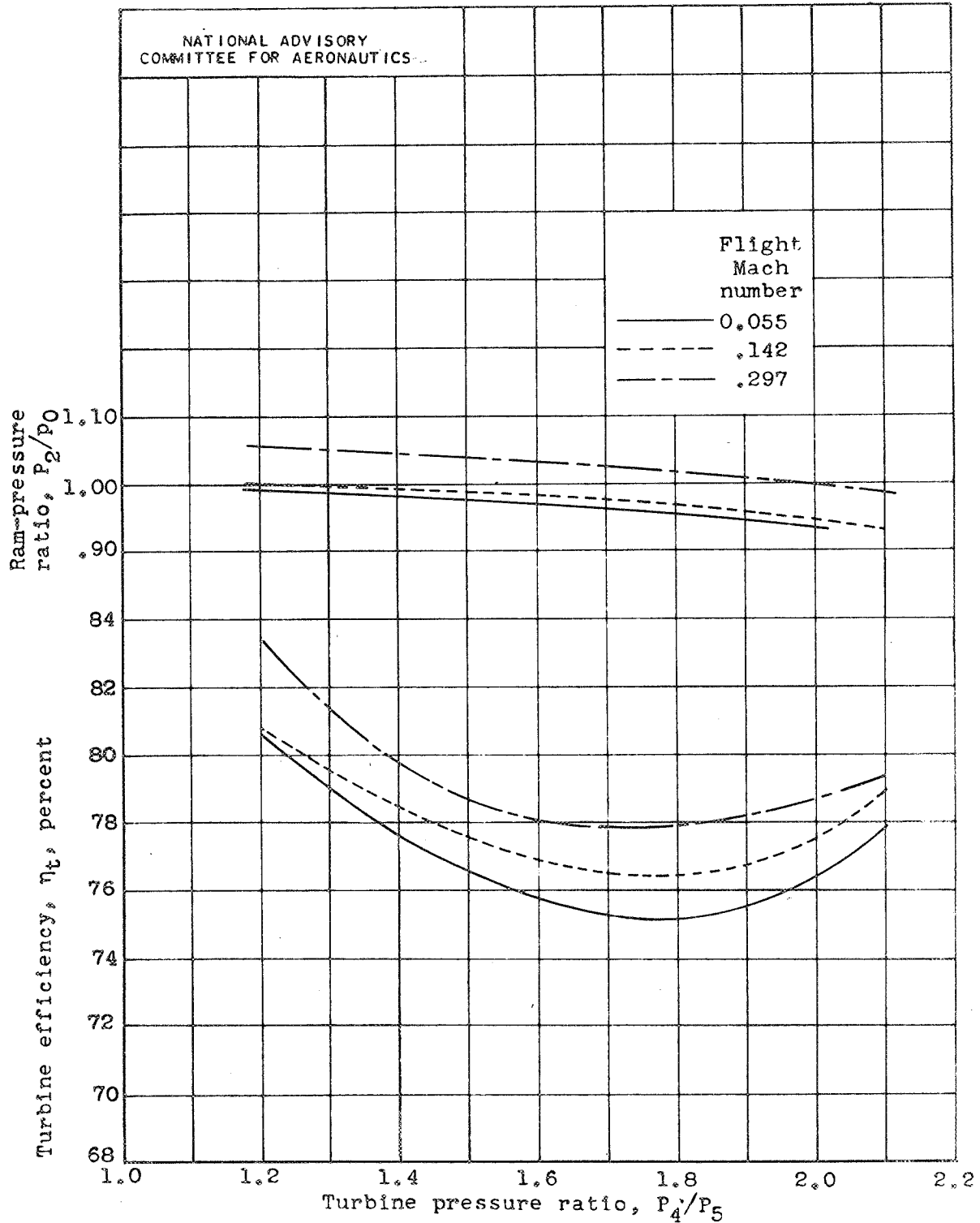


Figure 13.- Effect of flight Mach number on turbine efficiency. Simulated altitude, 5000 feet; tail cone in.